The American Journal of Pathology, Vol. 183, No. 3, September 2013

The American Journal of
PATHOLOGY
ajp.amjpathol.org

NEUROBIOLOGY

APOE3, but Not *APOE4*, Bone Marrow Transplantation Mitigates Behavioral and Pathological Changes in a Mouse Model of Alzheimer Disease

Yue Yang, Eiron Cudaback, Nikolas L. Jorstad, Jake F. Hemingway, Catherine E. Hagan, Erica J. Melief, Xianwu Li, Tom Yoo, Shawn B. Khademi, Kathleen S. Montine, Thomas J. Montine, and C. Dirk Keene

From the Department of Pathology, University of Washington, Seattle, Washington

Accepted for publication May 24, 2013.

Address correspondence to C. Dirk Keene, M.D., Ph.D., Harborview Medical Center, Box 359791, 325 Ninth Ave, Seattle, WA 98104. E-mail: cdkeene@uw.edu.

Apolipoprotein E4 (*APOE4*) genotype is the strongest genetic risk factor for late-onset Alzheimer disease and confers a proinflammatory, neurotoxic phenotype to microglia. Here, we tested the hypothesis that bone marrow cell *APOE* genotype modulates pathological progression in experimental Alzheimer disease. We performed bone marrow transplants (BMT) from green fluorescent protein—expressing human *APOE3/3* or *APOE4/4* donor mice into lethally irradiated 5-month-old *APPswe/PS1ΔE9* mice. Eight months later, *APOE4/4* BMT—recipient *APPswe/PS1ΔE9* mice had significantly impaired spatial working memory and increased detergent-soluble and plaque Aβ compared with *APOE3/3* BMT—recipient *APPswe/PS1ΔE9* mice. BMT-derived microglia engraftment was significantly reduced in *APOE4/4* recipients, who also had correspondingly less cerebral apoE. Gene expression analysis in cerebral cortex of *APOE3/3* BMT recipients showed reduced expression of tumor necrosis factor-α and macrophage migration inhibitory factor (both neurotoxic cytokines) and elevated immunomodulatory IL-10 expression in *APOE3/3* recipients compared with those that received *APOE4/4* bone marrow. This was not due to detectable *APOE*-specific differences in expression of microglial major histocompatibility complex class II, C-C chemokine receptor (CCR) type 1, CCR2, CX3C chemokine receptor 1 (CX3CR1), or C5a anaphylatoxin chemotactic receptor (C5aR). Together, these findings suggest that BMT-derived *APOE3*-expressing cells are superior to those that express *APOE4* in their ability to mitigate the behavioral and neuropathological changes in experimental Alzheimer disease. *(Am J Pathol 2013, 183: 905—917; http://dx.doi.org/10.1016/j.ajpath.2013.05.009)*

Humans uniquely have three different apolipoprotein E (*APOE*) alleles (ε2, ε3, and ε4). *APOE4* is the single greatest genetic risk factor for late-onset Alzheimer disease (AD), and there is a gene dosage effect.[1] However, genetic association does not inform function/pathogenesis. Multiple mechanisms have been postulated that predominantly focus on production, metabolism, or clearance of amyloid-β (Aβ) and that are variably supported by multiple observations, including: i) *APOE* genotype is strongly related to Aβ levels in brain and cerebrospinal fluid of AD patients[2,3]; ii) modulation of apolipoprotein E (apoE) protein levels in brain results in alterations of Aβ burden[4,5]; iii) Aβ degradation is at least partially apoE dependent[6,7]; and iv) Aβ clearance is differentially modulated by apoE isoforms, with *APOE*4 mice exhibiting reduced central and peripheral Aβ clearance compared with *APOE*3 mice.[8—10] Aβ degradation and clearance is at least partially dependent on microglia, the innate immune effector cells of the brain. Microglia have migratory and phagocytic capacity, are increased in the vicinity of Aβ plaques, and phagocytose Aβ.[11—13] *APOE* genotype modulates central nervous system innate immune function in culture,[14] including astrocyte and microglia elaboration of cytokines and chemokines,[15,16] microglia production of reactive oxygen species,[17] microglia-mediated paracrine neurotoxicity,[18] microglia migration,[19] and other functions.[20] However, the specific contribution of microglial *APOE* genotype to AD pathophysiology *in vivo* is largely unknown.

Supported by NIH grants P50AG05136, T32AG000258 (E.C., E.J.M.), and K01OD011072 (C.E.H.), and by the Nancy and Buster Alvord Endowment.

http://dx.doi.org/10.1016/j.ajpath.2013.05.009

To address this critical question and to test a potential therapeutic application, we used the fact that bone marrow transplantation (BMT) results in the gradual replacement of endogenous (host) microglia (to the near exclusion of other cell types) with microglia derived from donor marrow, in both wild-type mice and transgenic mouse models of AD.[21–24] We used targeted-replacement (TR) *APOE* mice homozygous for either the *APOE*3 or *APOE*4 gene inserted into the mouse *APOE* regulatory elements[25,26] that coexpressed green fluorescent protein (GFP). We transplanted whole bone marrow (BM) isolated from TR *APOE3/3*;GFP or TR *APOE4/4*;GFP mice into lethally irradiated *APPswe/PS1ΔE9* mice to determine the specific role of microglial *APOE* genotype in the pathological progression of AD.

Materials and Methods

Animals

Transgenic Mice

BMT were performed in host double-transgenic *APPswe/PS1ΔE9* mice using TR *APOE3/3*;GFP or TR *APOE4/4*;GFP mice as donors. The *APPswe* transgene encodes a mouse–human hybrid transgene containing the mouse sequence in the extracellular and intracellular regions and a human sequence within the Aβ domain with Swedish mutations K594N and M595L. The *PS1ΔE9* transgene encodes exon-9–deleted human presenilin-1. Both transgenes are coexpressed under control of the mouse prion promoter, with plaque deposition beginning at approximately 5 months of age.[27,28] TR *APOE* mice are homozygous for replacement of mouse *apoE* gene with the human *APOEε3* (*APOE3*) or *APOEε4* (*APOE4*) allele backcrossed onto a C57BL/6 genetic background,[25,26] expressing human isoforms apoE3 or apoE4 under control of mouse regulatory elements. GFP mice (C57BL/6 background) were intercrossed with *APOE3/3* or *APOE4/4* animals to generate homozygous GFP mice that were also homozygous *APOE3/3* or *APOE4/4*. GFP expression is under control of the β-actin promoter and cytomegalovirus enhancer. All mouse strains were purchased from the Jackson Laboratory (Bar Harbor, ME) and maintained on a C57BL/6 background. Mice were housed in standard laboratory conditions with a strict 12-hour light/dark cycle and with free access to mouse chow and water. All mice were used with approval of the University of Washington Animal Care and Use Committee.

Generation of Chimeric Mice

BMT was performed according to our previously published protocols.[24] Host *APPswe/PS1ΔE9* double-transgenic mice at 5 months of age received total-body 10.5-Gy single-dose irradiation at approximately 2 Gy per minute from a cesium-137 source (Model 81-14; JL Shepherd, San Fernando, CA). BM cells were isolated from 8-week-old male *APOE3/3*;GFP or *APOE4/4*;GFP transgenic mice by flushing the femur and tibias with RPMI media with 10% fetal bovine serum. The samples were combined, passed through a 25-G needle filtered through a 70-μm nylon mesh, and centrifuged. Erythrocytes were lysed in ammonium chloride potassium buffer (Invitrogen, Carlsbad, CA), and the remaining leukocytes were resuspended in sterile PBS at a concentration of approximately 5×10^6 viable nucleated cells per 200 μL. Irradiated *APPswe/PS1ΔE9* mice received *APOE3/3*;GFP ($n = 11$) or *APOE4/4*;GFP ($n = 8$) bone marrow cells (BMCs) via retro-orbital venous plexus injections 1 day after total-body irradiation and were housed in autoclaved cages. Chimeric mice underwent behavioral testing 8 months after transplantation and were then euthanized for tissue analysis.

Primary Cell Cultures

Microglia or astrocytes (*APOE3/3* or *APOE4/4*) were isolated and purified from neonatal mouse cortex following established procedures[29,30] and plated at 2.5×10^4 cells per well in 96-well plates. Following 24 hours culture, the cells were incubated in serum-free medium for an additional 18 hours. The conditioned medium was collected and apoE protein levels were measured by an enzyme-linked immunosorbent assay (ELISA) following the manufacturer's protocol (Mabtech AB, Cincinnati, OH). In brief, 100 μL of conditioned medium (dilution 1:10) was loaded in 96-well plates precoated with an anti-apoE antibody and incubated for 1.5 hours at room temperature. The plates were rinsed in PBS. A biotinylated detection antibody was added. After 1 additional hour incubation and rinsing, streptavidin–horseradish peroxidase was added for 1-hour incubation. Tetramethylbenzidine substrate solution was added, followed by stop solution. Optical density was read at a wavelength of 450 nm.

Behavioral Analysis

Open Field

Locomotor activity and habituation to a novel environment were measured using an open field test. Mice of each group were tested in the same session. Each mouse was placed in the center of the open field apparatus (40 × 40 × 30 cm; San Diego Instruments, San Diego, CA). The bottom was demarcated into a 5 × 5 grid making 25 equal-sized (8 × 8 cm) squares. Mice were allowed to explore the open field arena undisturbed for 5 minutes. This was repeated for 6 days. Videos were scored by an experimenter (C.E.H.) blind to the study, for total distance traveled using AnyMaze software version 4.2 (Stoelting Company, Wood Dale, IL). A decrease in distance traveled over repeated trials is indicative of recognition of and habituation to the novel testing environment.

Barnes Maze

We used a modified Barnes maze protocol to assess hippocampal-dependent spatial learning and memory. The

Barnes maze apparatus (San Diego Instruments) is a disk 1.0 m in diameter raised 75 cm off the floor containing 18 possible escape holes, one of which leads to a dark escape box. Bright light and fan noise were used to increase motivation for escape. Animals were trained to escape the maze into the hidden box by allowing them to explore the maze for 60 seconds and then placing them in the box with a food pellet before any testing. Animals were then trained over a 3-day acquisition phase to learn the location of the escape box within the maze using spatial cues (three trials per day with a 2-minute intertrial interval). Trials ended when animals found the escape box or 300 seconds had elapsed. After day 3, to increase the cognitive load on the animals and engage working memory, the escape box was moved to a different randomized location, and animals were again given three trials to learn the new location (2-minute intertrial interval) in a reversal learning scenario. Latency to escape, distance traveled, and errors made (investigations into decoy escape holes) were measured (AnyMaze). The number of errors mice made in finding the escape box was modeled as a Poisson distribution. Search strategies were classified as random search, serial search, and spatial search.[31] An overall frequency was calculated for each type of strategy for each mouse.

Tissue Collection and Processing

Animals were anesthetized with 2.5% tribromoethanol (Avertin; Sigma-Aldrich, St. Louis, MO) 8 months post transplantation. Blood was drawn via cardiac puncture and processed for complete blood counts and flow cytometry before the mice were transcardially perfused with ice-cold PBS. Brains were rapidly removed from the skulls and divided by mid-sagittal section. One hemibrain was dissected into anatomically distinct regions (including rostral and caudal cerebral cortex, striatum, hippocampus, cerebellum, thalamus/midbrain, and brainstem). The caudal cortex fragment was immediately placed in cold HBSS and processed for microglia isolation and quantitation of central engraftment and microglia molecular phenotype by flow cytometry. The rostral cortex was divided into an RNA fraction (>15 mg) and a protein fraction, and along with the other regions, immediately flash frozen in liquid nitrogen and stored at −80°C for mRNA or protein quantification. Total hippocampus from each mouse was required for effective quantitation of Aβ and apoE (*Protein Extraction, Aβ, and apoE Quantification*), which thus precluded hippocampal RNA isolation, and therefore, hippocampal cytokine analysis. The contralateral hemibrain was post-fixed for 2 days in 4% paraformaldehyde (pH 7.6) and then placed in PBS solution containing 30% (w/v) sucrose for 2 days at 4°C. The frozen brains were embedded in optimal cutting temperature compound, frozen in liquid isopentane, and then coronally sectioned in 40 μm increments using a cryostat (Leica CM3050; Leica, Wetzlar, Germany). Slices were collected in cold cryoprotectant solution [0.05 mol/L sodium phosphate buffer (pH 7.3), 30% ethylene glycol, and 20% glycerol] and stored at −20°C until needed for immunostaining.

Microglia Isolation

Microglia/monocytes were isolated from brain homogenates as described previously, with some modifications.[32] Briefly, caudal cerebral cortex was dissociated by gentle homogenization in HBSS. The cells were then incubated with HBSS containing 15 U/mL papain, 100 μg/mL DNase, and 0.5 mmol/L EDTA (pH 7.4) for 20 minutes at 37°C. The cell suspension was passed through a 70-μm nylon cell strainer and centrifuged at 300 × *g* for 7 minutes. Supernatant was removed, and cell pellets were resuspended in 70% isotonic Percoll (GE Healthcare, Uppsala, Sweden). A discontinuous Percoll density gradient was set up as follows: 70%, 35%, and 0% isotonic Percoll. The gradient was centrifuged for 30 minutes at 1200 × *g*. Mononuclear phagocytes were collected from the interphase between the 70% and 35% Percoll layers.[33] Cells were washed and then resuspended in HBSS for staining.

Flow Cytometry

Peripheral engraftment and differentiation of GFP^+ donor BM-derived cells were assessed by flow cytometry of peripheral blood. Red blood cells were removed using lysis buffer (Sigma-Aldrich). Cells were then washed several times in buffer solution (HBSS containing 2% fetal bovine serum) and incubated with antibodies on ice for 30 minutes. Cells were fixed with 1% paraformaldehyde and then analyzed using an LSR II flow cytofluorometer (BD Biosciences, Franklin lakes, NJ). Identically processed blood from GFP and wild-type mice was used as controls. Peripheral (blood) engraftment was determined as a percentage of GFP^+ cells divided by the total number of nucleated cells. Multilineage differentiation of donor BMCs was determined by staining with eFluor 450−conjugated CD3 (T cells), PerCP-Cy5.5−conjugated CD19 (B cells), allophycocyanin (APC)-conjugated Gr-1 (neutrophils), and phycoerythrin (PE)-conjugated CD11b (monocytes/macrophages) antibodies (eBioscience, San Diego, CA). Appropriately labeled IgG isotype control antibodies were used as negative controls.

For central nervous system (CNS) engraftment, flow cytometric analysis was performed on mononuclear cells (*vide infra*) isolated from cerebral cortex. The cells were washed and then stained with PE-Cy7−conjugated CD11b and Alexa Fluor 700−conjugated CD45 antibodies for 60 minutes. The cell suspension was analyzed to identify the population of $CD11b^+CD45^{low}$ microglia.[34–36] Central (cerebral cortex) engraftment of BM-derived microglia was determined by dividing the $CD11b^+CD45^{low}GFP^+$ cell population by total $CD11b^+CD45^{low}$ microglia. The assessment of cell-surface protein expression was performed using eFluor 450−conjugated major histocompatibility

complex (MHC) class II (eBioscience), APC-conjugated C-C chemokine receptor type 1 (CCR1), PE-conjugated CCR2 (R&D Systems, Minneapolis, MN), or Alexa Fluor 647–conjugated C5a anaphylatoxin chemotactic receptor (C5aR, alias CD88) (AbD Serotec, Kidlington, UK) antibody. After washing, the cells were incubated with the fluorescent-labeled primary antibody or IgG isotype control for 60 minutes at 4°C. For CX3C chemokine receptor 1 (CX3CR1) detection, washed cells were first incubated with monoclonal antibody anti-CX3CR1 (Abcam, Cambridge, MA) or IgG isotype control for 60 minutes on ice. After washing, cells were incubated for 60 minutes with a PerCP-conjugated anti-rat polyclonal antibody (Jackson Immunoresearch, West Grove, PA). The expression of MHC class II, CCR2, and CX3CR1 was assessed as mean fluorescence intensity in GFP^+ and GFP^- microglia populations. All flow cytometry experiments were performed using a four-laser and 12-color flow cytofluorometer LSR II (BD Biosciences). Data were analyzed with FlowJo software version 7.2.2 (Tree Star, Ashland, OR).

Immunofluorescence and Stereological Analysis

Every sixth coronal section was used for immunostains and unbiased stereological methods (13 months of age, $n = 8$ to 11 per group). Immunofluorescence staining was performed according to previously published protocols.[24] Primary antibodies included anti–Iba-1 (dilution 1:500; Wako, Richmond, VA) and anti-Aβ 1-16 peptides (dilution 1:1000; 6E10;Covance, Princeton, NJ); species-appropriate secondary antibodies were conjugated to Cy3 (dilution 1:400; Jackson Immunoresearch). Prolong-gold anti-fade with DAPI (Invitrogen) was used for coverslipping and nuclear counterstain. All images were captured using an FV1000 laser scanning confocal microscope (Olympus, Center Valley, PA).

To quantify ionized calcium binding adaptor molecule 1–positive ($Iba\text{-}1^+$) microglia and BM-derived mononuclear cells (GFP^+), sections were analyzed using unbiased stereological cell quantification using systematic random sampling. Every sixth brain section (240 μm apart) was analyzed at ×400 magnification using a Nikon inverted fluorescence microscope (Melville, NY) and Stereo Investigator software version 7.52 (MBF Bioscience, Williston, VT). An optical fractionator was used with a counting frame measuring 150 μm × 150 μm applied every 500 μm in hippocampus and every 750 μm in cortex. Cells were assessed as $Iba\text{-}1^+$, GFP^+, or $Iba\text{-}1^+$ and GFP^+ double immunopositive. All analysis was performed by operators blinded to experimental conditions (N.L.J. and Y.Y.).

Immunohistochemistry and Plaque Assessment

To assess Aβ plaques, every sixth section (average, 15 per mouse) was processed for immunohistochemistry using a rabbit polyclonal anti–pan Aβ antibody (dilution 1:750; Invitrogen) according to our previously published protocol.[24] Brain sections were immersed in Tris-buffered saline (50 mmol/L Tris, 138 mmol/L NaCl, 2.7 mmol/L KCl). Endogenous peroxidase in tissue was quenched by treating with 30% methanol and 1% H_2O_2 in PBS for 2 minutes at room temperature. Nonspecific background staining was blocked by incubation in 10% donkey serum, 2% bovine serum albumin with 0.5% Triton X-100, and 0.1% azide in Tris-buffered saline for 3 hours. Sections were then incubated with primary antibody overnight at 4°C, rinsed three times with Tris-buffered saline, and then incubated with biotinylated secondary antibody followed by ABC kit reagent (Vector Laboratories, Burlingame, CA) for 2 hours each. Finally, the sections were incubated for exactly 3 minutes with diaminobenzidine (DAB) (Sigma-Aldrich). After washing, the sections were mounted on slides, dehydrated in a series of graded ethanol, cleared with Citri-Solv, and then coverslipped with Permount mounting medium (Fisher Scientific, Pittsburgh, PA).

Stained sections were photographed (Nikon Super Coolscan 4000 ED), and the digital images were analyzed separately for cerebral cortex and hippocampus using ImageJ software version 1.46r (NIH, Bethesda, MD). Total area of immunoreactivity was determined using a standardized histogram-based threshold technique. The percent area occupied by Aβ-immunoreactive plaques, as well as the plaque size and numbers, was averaged over all sections for each mouse, and averaged values from each mouse were used in statistical analysis. The operator (J.F.H.) was blinded to experimental conditions.

Protein Extraction, Aβ, and apoE Quantification

Proteins from rostral cortex and total hippocampus were extracted using a modified version of previously published procedures.[24,37,38] All manipulations were performed on ice to minimize protein degradation. Tissue was weighed and placed in an Eppendorf tube containing Tris-HCl buffer [20 mmol/L Tris-HCl (pH 7.5), 150 mmol/L NaCl, 1 mmol/L phenylmethylsulfonyl fluoride, and protease cocktail inhibitor tablet (Roche, San Francisco, CA)] at a concentration of 10 μL/mg and was then sonicated on ice three times for 10 seconds at a time. After 30 minutes centrifugation at 30,000 × g at 4°C, the supernatant (soluble fraction) was collected and frozen at −80°C. The insoluble pellet was resuspended in 5 mol/L guanidine-HCl buffer with the same volume as Tris-HCl buffer followed by 30 minutes centrifugation at 30,000 g at 4°C. The supernatant (insoluble fraction) was collected and frozen at −80°C. Quantification of soluble and insoluble $A\beta_{40}$ and $A\beta_{42}$ was performed using human Luminex kits (Invitrogen) according to the manufacturer's protocol. Tris-HCl soluble cortical and hippocampal fractions from chimeric mice were generated as described above and assayed for apoE using a commercially available human apoE ELISA per the manufacturer's protocol (#3712-1H-6; Mabtech AB). The monoclonal capture antibody shows cross-reactivity with mouse apoE.

qPCR

Total RNA was extracted from rostral cortex of chimeric mice at 8 months after BMT using the RNeasy kit (Qiagen, Valencia, CA) according to the manufacturer's suggestions. Each cohort of 8 to 11 mice was analyzed for mRNA levels of chemokine ligand 2 (CCL2), chemokine (C-X3-C motif) ligand 1 (CX3CL1), IL-6, tumor necrosis factor-α (TNF-α), IL-4, IL-10, macrophage migration inhibitory factor (MIF), and CCL8 with real-time quantitative PCR (qPCR). One microgram of total RNA was reverse-transcribed using a RETROscript kit (Ambion, Austin, TX). The cDNA synthesized from total RNA was diluted 10-fold with DNase-free water, and each cDNA sample was independently tested three times. Transcript quantities were assayed by TaqMan gene expression assay (Applied Biosystems, Foster City, CA): CCL2 (ID Mm00441242_m1), CX3CL1 (ID Mm00436454_m1), IL-6 (ID Mm00446190_m1), TNF-α (ID Mm00443260_g1), IL-4 (ID Mm00445259_m1), IL-10 (ID Mm00439614_m1), MIF (ID Mm01611157_gH), and CCL8 (ID Mm01297183_m1) were assayed in a model 7300 real-time PCR system (Applied Biosystems). Cycling conditions of the real-time PCR were 95°C for 20 seconds, 40 cycles of 95°C for 1 second, and 60°C for 20 seconds. Mouse 18s ribosomal RNA (ID Mm03928990_g1) expression was used as an endogenous control. qPCR was performed according to the guidelines provided by Applied Biosystems. The comparative cycle threshold (C_T) method ($\Delta\Delta C_T$ quantitation) was used to assess the difference between samples. Quantitative data analysis followed the suggestions of the manufacturer.

Statistical Analysis

Results are expressed as means ± SEM. Statistical analysis was performed by the unpaired Student *t*-test or one- or two-way analysis of variance as indicated. Post hoc testing used the Bonferroni method. Statistical significance was assumed if $P < 0.05$. All statistical analyses were performed using GraphPad Prism software version 5.03 (San Diego, CA).

Results

Generation of TR *APOE3/3*;GFP and TR *APOE4/4*;GFP *APPswe/PS1ΔE9* Chimeras

BM from TR *APOE3/3*;GFP or TR *APOE4/4*;GFP donor mice was transplanted into 5-month-old *APPswe/PS1ΔE9* recipient mice 24 hours after myeloablative (10.5 Gy) whole-body irradiation. The resulting *APOE3/3*;GFP and *APOE4/4*;GFP *APPswe/PS1ΔE9* chimeras underwent behavioral testing at 8 months post-BMT and were then euthanized. Blood was collected by cardiac puncture at the time of sacrifice, and complete blood counts with differentials were performed; white blood cell, red blood cell, and platelet counts did not differ between groups (Supplemental Figure S1, A–C). Multilineage differentiation of hematopoietic stem cells was within the normal range, with no significant differences between groups (Supplemental Figure S1D).

Hematopoietic Engraftment by *APOE3/3* or *APOE4/4* Donor Cells

To determine BM engraftment, GFP^+ cells in the chimeras were analyzed by flow cytometry. As expected, almost all blood mononuclear cells were GFP^+, and there was no difference in total peripheral engraftment between donor genotypes (Figure 1A). Using lineage-specific antibodies, we next analyzed the mononuclear cell composition to compare differentiation into hematopoietic lineages in hematopoietic stem cells. We found no differential influence of *APOE* on the proportions of T and B lymphocytes and neutrophils (Figure 1B). Interestingly, although differential blood counts revealed no differences in total monocytes (Supplemental Figure S1D), flow cytometry of peripheral blood showed *APOE4/4* BMT gave rise to fewer $CD11b^+$ monocytes/macrophages than did *APOE3/3* BMT ($P < 0.05$) (Figure 1B), suggesting effects of *APOE* on monocyte molecular phenotype in the periphery. Representative flow cytometric contours for each hematopoietic lineage are shown in Figure 1C.

Increased CNS Microglia/Monocyte Engraftment by *APOE3/3* versus *APOE4/4* Donor Cells

We next determined microglia density and CNS engraftment in both chimeras. Mononuclear cells were isolated for flow cytometry from cerebral cortex and were then probed for microglia, which, unlike peripheral monocytes, are CD11b-positive ($CD11b^+$) and CD45-low expressing ($CD45^{low}$) cells.[39] Although almost half of the $CD11b^+CD45^{low}$ cells were BMT derived (GFP^+) in *APOE3/3* recipients, less than a third of microglia in *APOE4/4* recipients were derived from the donor transplant ($P < 0.01$) (Figure 2A). Flow cytometric contours from representative mice are presented in Figure 2B.

To further quantitate *APOE* genotype effects on BMT-derived monocyte/microglia engraftment and to evaluate microglia morphology, we analyzed hippocampus and cerebral cortex from the contralateral hemisphere using immunofluorescence histology. BMT-derived cells were identified by strong GFP autofluorescence in both groups, and on the basis of Iba-1 immunopositivity, were almost uniformly microglia (Figure 3A). Donor and host microglia in both groups were mostly classically ramified, with some $Iba\text{-}1^+$ cells showing blunted processes and enlarged somas. However, macrophage/amoeboid morphology was not identified in $Iba\text{-}1^+$ cells from either group. Unbiased stereological analysis revealed significantly increased donor-derived microglia in *APOE3/3* compared to *APOE4/4* recipients in cerebral cortex (55.2 ± 4.0% *APOE3/3* versus 39.3 ± 5.6% *APOE4/4*; $P < 0.05$) and in hippocampus (63.0 ± 3.9% *APOE3/3* versus 44.9 ± 5.0% *APOE4/4*; $P < 0.05$) (Figure 3B). Overall,

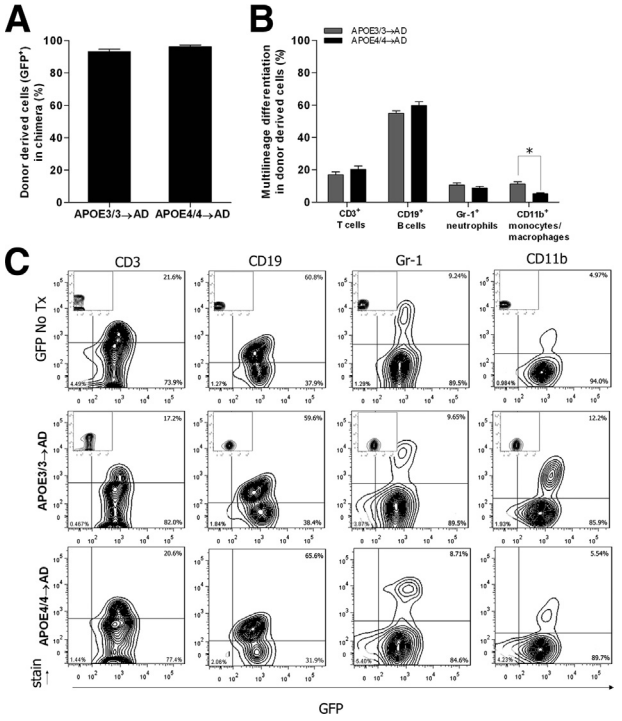

Figure 1 Peripheral (blood) engraftment and hematopoietic reconstitution in BMT recipients. **A:** Percent peripheral engraftment was calculated by comparing GFP^+ leukocytes to total leukocytes using flow cytometry, and revealed nearly complete peripheral engraftment with no significant donor genotype differences detected. **B:** Flow cytometric analysis of peripheral blood for hematopoietic lineage differentiation of GFP^+ BMT-derived cells. GFP fluorescence was measured in T lymphocytes, B lymphocytes, neutrophils, and monocytes/macrophages, and revealed a significant influence of donor *APOE* genotype on the percentage of donor-derived monocytes. $^*P < 0.05$, two-way analysis of variance analysis using the Bonferroni *post hoc* test. All results are expressed as means ± SEM, $n = 8$ to 11. **C:** Flow cytometric analysis of peripheral blood of representative mice stained with antibodies to the fluorophore-conjugated T-cell marker CD3, B-cell marker CD19, neutrophil marker Gr-1, and CD11b (to stain the monocytes and macrophages). GFP intensity (marking donor cells) is plotted on the *x* axis, and the intensity of the stain with lineage-specific markers of hematopoietic differentiation is plotted on the *y* axis. Positive graph shows the pattern of a nontransplanted GFP mouse (GFP No Tx). Negative graph (GFP No Tx, **inset**) shows autofluorescence pattern of a nontransplanted wild-type mouse; iso graph (*APOE3/3*;GFP→AD, **inset**) shows isotype-matched nonspecific antibody staining of the transplanted mouse.

cerebral cortical and hippocampal microglia densities (expressed as Iba-1^+ cells per mm^3) were not significantly different between the two groups in the cortex or hippocampus, and there was no significant *APOE* effect on total microglia density between BM recipients (Figure 3C). Taken together, flow cytometric and stereological data suggest that *APOE3/3* donor monocytes are more efficiently engrafted in the brain than *APOE4/4* donor monocytes.

Increased CNS apoE Concentration in *APOE3/3* Recipient Mice

Because *APOE3/3* recipients had increased densities of BMT-derived microglia, we determined whether BMT using donor marrow from mice expressing human *APOE3* or *APOE4* might modulate brain apoE levels in cerebral cortex and hippocampus. *APOE3/3* transplantation resulted in 45 ± 8% greater cerebral cortical apoE protein levels than did *APOE4/4* ($P < 0.001$) (Figure 4). A similar change (40 ± 11% greater apoE) was observed in the hippocampus of *APOE3/3* recipients ($P < 0.01$) (Figure 4).

Others have demonstrated in primary cultures of mixed glia that microglia, especially under conditions of innate immune activation, contribute a substantial proportion of secreted apoE.[40] We further pursued apoE isoform glial secretion in primary cultures of microglia or astrocytes prepared from *APOE* mice (Figure 5). Under basal culture conditions, which likely represent at least mild activation compared to *in vivo*, *APOE3/3* primary astrocyte cultures secreted more apoE than did *APOE4/4* astrocytes. Primary microglia cultures from the same mice secreted comparable amounts of apoE as astrocytes but with the opposite isoform-specific relationship: *APOE4/4* secretion was greater than that of *APOE3/3* (Figure 5). Importantly, two-way analysis of variance for these data showed a significant interaction between *APOE* and glial cell type ($P < 0.01$).

Improved Habituation and Spatial Working Memory in *APOE3/3*;GFP Recipients

Open field and Barnes maze behavior test data were analyzed for *APOE*-dependent effects. Nontransplanted

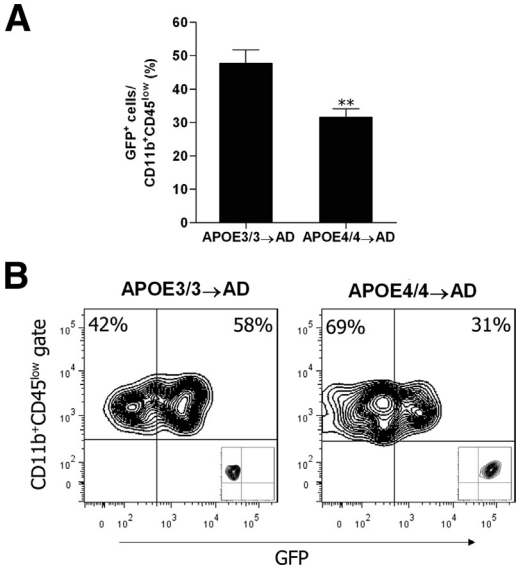

Figure 2 Flow cytometric analysis of cerebral cortical engraftment of BMT-derived microglia. Mononuclear cells were isolated (dissociation with Percoll gradient) from rapidly dissected cerebral cortex from *APPswe/PS1ΔE9* mice transplanted with *APOE3/3*;GFP or *APOE4/4*;GFP BMCs 8 months post-transplantation after transcardial perfusion with ice-cold PBS. **A:** Engraftment of $GFP^+CD11b^+CD45^{low}$ microglia was increased in *APOE3/3*;GFP compared with *APOE4/4*;GFP recipient *APPswe/PS1ΔE9* mice. $^{**}P < 0.01$, unpaired Student's *t*-test. **B:** Representative flow cytometric contours of GFP fluorescence (*x* axis) in $CD11b^+CD45^{low}$ gate (*y* axis) are shown for population of host (GFP^-) versus donor (GFP^+) microglia. Negative graph (*APOE3/3*→AD, **inset**) shows the pattern of a nontransplanted wild-type mouse. Positive graph (*APOE4/4*→AD, **inset**) shows the pattern of a nontransplanted GFP mouse.

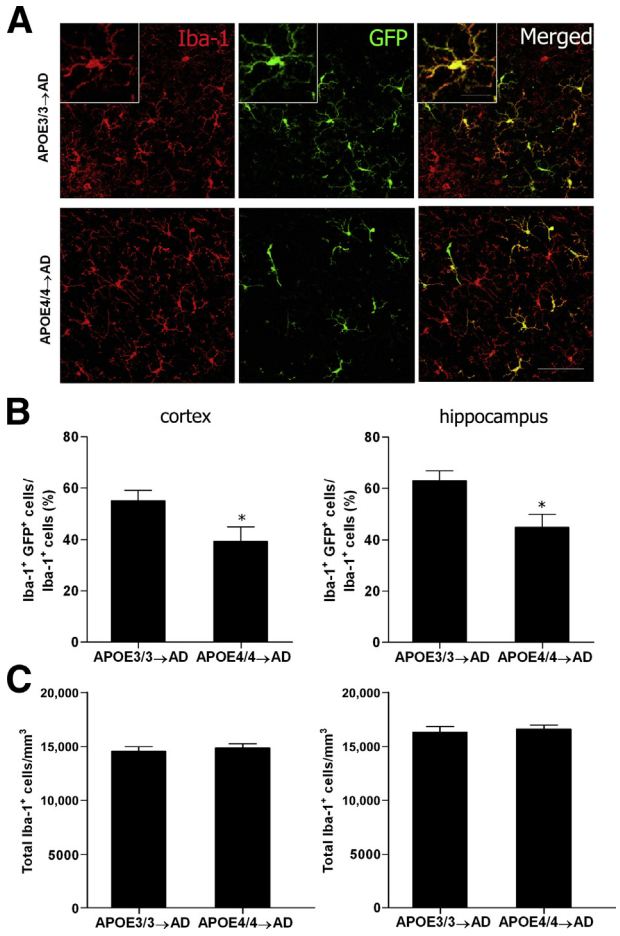

Figure 3 Cortex and hippocampal microglia in BMT-recipient mice. Iba-1 immunostaining was performed on 40-μm sections from 13-month-old *APPswe/PS1ΔE9* mice sacrificed 8 months post-BMT. **A:** Iba-1 immunoreactivity (red) for microglia shows no clear difference in total microglia between groups and highlights predominantly ramified morphology in both groups. Fluorescence microscopy reveals an increased density of GFP^+ cells (GFP, green, **inset**) in the cortex of *APOE3/3*;GFP→*APPswe/PS1ΔE9* mice compared with *APOE4/4*;GFP→ *APPswe/PS1ΔE9* mice. Merged images confirm that GFP^+ cells are also uniformly Iba-1^+ and therefore of donor origin, whereas others represent endogenous microglia and only express Iba-1. Scale bars: 50 μm; 10 μm (**insets**). **B:** Unbiased stereological analysis of BMT-derived microglia engraftment in the cortex and hippocampus of chimeric mice reveals proportionately increased engraftment in *APOE3/3*;GFP recipients compared with *APOE4/4*;GFP recipients. $*P < 0.05$, unpaired Student *t*-test. **C:** Quantitative analysis of microglia cell density (total Iba-1^+ microglia/mm^3) in the cortex and hippocampus of chimeric mice shows no evidence of *APOE* genotype effect on total microglia. Error bars show the means ± SEM, $n = 8$ to 10.

APPswe/PS1ΔE9 mice demonstrated behavior consistent with that previously reported by others in both tests.[41,42] *APOE3/3* mice showed habituation to a novel environment as seen by a progressive reduction in total distance traveled over successive days ($P < 0.05$) (Figure 6A). By contrast, *APOE4/4* mice showed no significant reduction in distance traveled over successive days. There was no significant difference ($P > 0.05$) in baseline locomotor function between the two groups, nor were there any significant differences ($P > 0.05$) in the acquisition phase of the Barnes maze test;

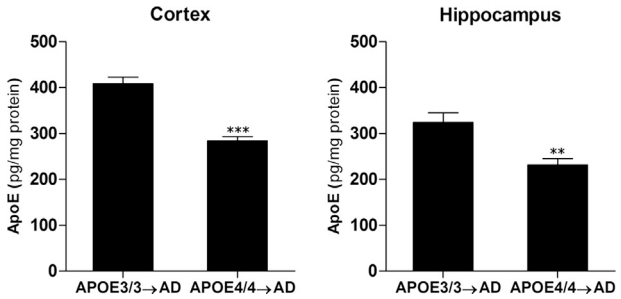

Figure 4 Effect of donor *APOE* genotype on cerebral apoE concentration. Cortex and hippocampus Tris-HCl buffer lysates from 13-month-old *APPswe/PS1ΔE9* mice that received BMT from *APOE3/3*;GFP or *APOE4/4*;GFP donor mice 8 months before sacrifice were subjected to ELISA for apoE. There was significantly increased apoE concentration in mice that received *APOE3/3*;GFP BMT compared with *APOE4/4*;GFP recipients in both cortex and hippocampus. $**P < 0.01$, $***P < 0.001$, Student's *t*-test.

however, reversal learning was significantly ($P < 0.05$) preserved in *APOE3/3* BM recipients compared with *APOE4/4* recipients. *APOE3/3* mice exhibited reduced distance traveled ($P < 0.01$) (Figure 6, B and C), shorter escape latency ($P < 0.01$) (Figure 6D), and fewer errors ($P < 0.01$) (Figure 6E) than *APOE4/4*mice. Characterization of search strategy in the Barnes maze can provide insight into functional impairment.[31] Analysis of videos from each mouse for each trial revealed that the *APOE3/3* BM recipients used a predominantly (33%) spatial search strategy, whereas the *APOE4/4* group used a predominantly (42%) random one (Figure 6F). These *APOE4/4* recipients only used a spatial or serial search strategy 16% of the time, whereas *APOE3/3* recipients used one of these strategies 50% of the time (Figure 6F). These data demonstrate better spatial working memory in *APPswe/PS1ΔE9* recipients of *APOE3/3* versus *APOE4/4* BMT. Given these *APOE*-specific differences in behavior, we next explored cellular and biochemical changes in the brains of these mice.

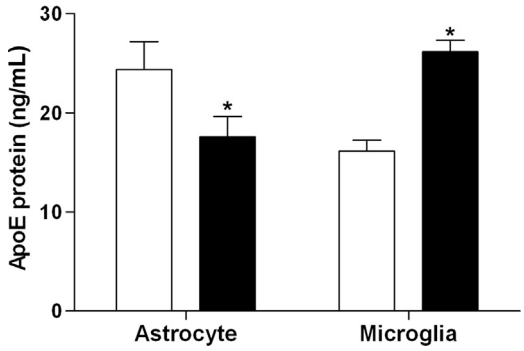

Figure 5 Primary cultures of mouse astrocytes or microglia were prepared from neonatal TR *APOE3/3* (white bars) or *APOE4/4* (black bars) mice and plated at 2.5×10^4 cells per well in 96-well plates. Following 24 hours in culture, the medium was replaced with serum-free medium. After 18 hours in culture, the conditioned medium was assayed for apoE concentration by ELISA. Two-way analysis of variance (df 1,1,40) had $P < 0.01$ for interaction between *APOE* and glial cell type, but was not significant for either *APOE* or glial cell type. $*P < 0.05$ for *APOE3/3* versus *APOE4/4* in astrocyte and in microglia conditioned medium, Bonferroni-corrected post-test comparisons.

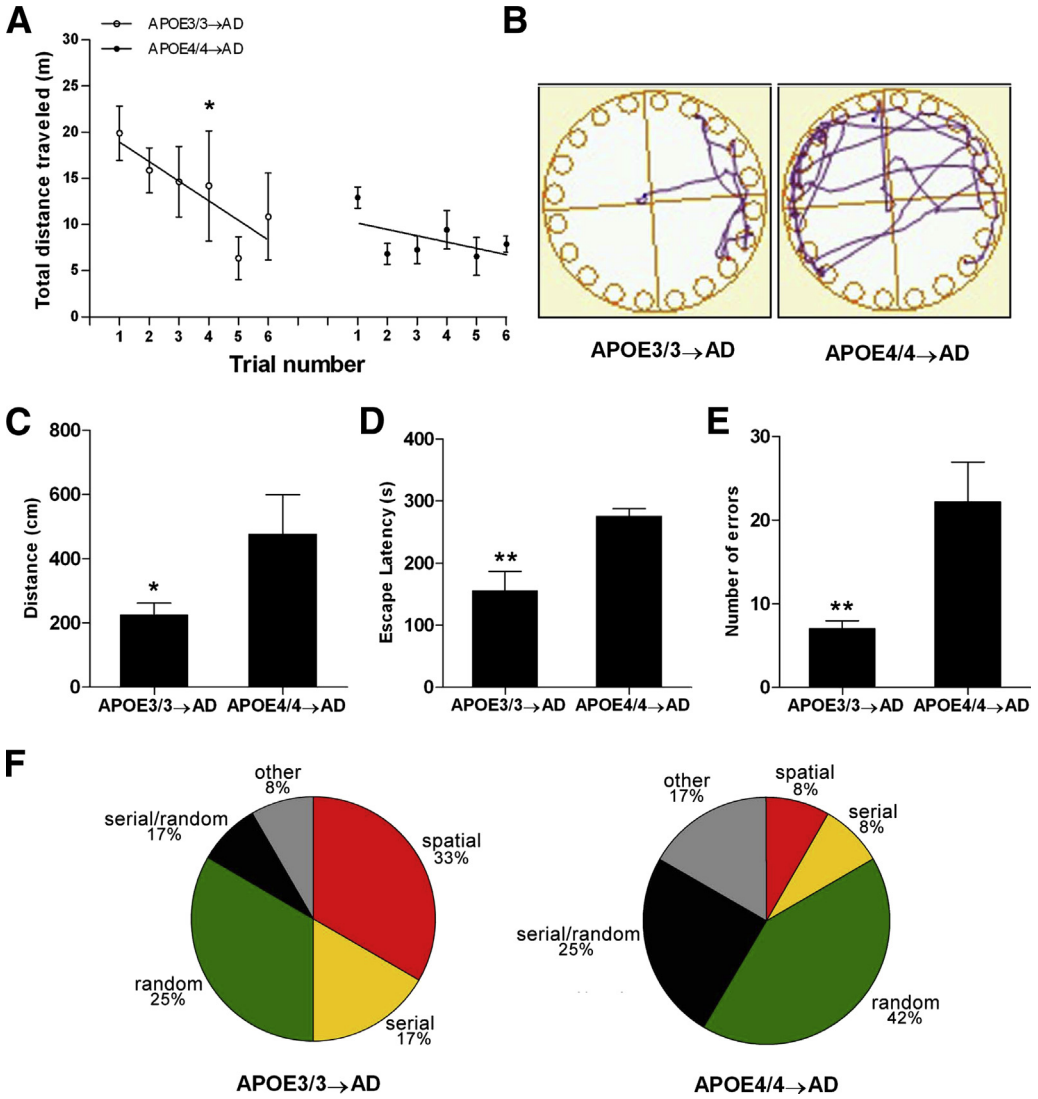

Figure 6 *APOE3/3*;GFP BMT mitigates behavioral deficits in *APPswe/PS1ΔE9* mice. **A**: Open field: as a proxy for cognitive function, habituation to an open field was analyzed by determining whether total distance traveled decreased as a function of time (trial day). Linear regressions were performed. Slopes significantly different from zero were interpreted as normal cognition, because distance is expected to decrease with subsequent testing in cognitively normal animals. $^{*}P < 0.05$. Results are expressed as means ± SEM, $n = 8$ to 10. **B**–**E**: Barnes maze: 13-month-old *APOE3/3*;GFP BMT–recipient *APPswe/PS1ΔE9* mice exhibited preserved cognitive function compared with *APPswe/PS1ΔE9* mice that received *APOE4/4*;GFP BMT. After a 3-day training session, the escape location was switched and the mice tested over three trials to find the new location. **B**: The track plots represent paths traveled during challenge trials of the chimeric mice. *APOE3/3*;GFP BMT recipients traveled a shorter distance (**C**), required less time (**D**), and made fewer errors (**E**) than *APOE4/4*;GFP BMT recipients. $^{*}P < 0.05$, $^{**}P < 0.01$, Student *t*-test. All results are expressed as means ± SEM. **F**: Videos of each mouse from each challenge trial were scored for the percent time spent with specific search strategies revealing that *APOE3/3*;GFP BMT recipients used serial (yellow) and spatial (red) search strategies 50% of the time, compared to 16% for *APOE4/4*;GFP BMT recipients.

Reduced CNS Aβ in *APOE3/3*;GFP-Recipient *APPswe/PS1ΔE9* Mice

One possible cause of preserved behavioral performance in *APOE3/3* than *APOE4/4* BM recipients is suppression of Aβ accumulation in brain as a result of more efficient engraftment of cerebral cortex and hippocampus. To test this possibility, we first quantified Aβ plaque burden (total area occupied by plaque, plaque frequency, and mean plaque size) in hippocampus and cortex from both groups using a standard thresholding technique on coronal sections that had been immunohistochemically stained with a pan-Aβ antibody (Figure 7A). Total area occupied by Aβ plaques (2.9% *APOE3/3* versus 3.9% *APOE4/4*; $P < 0.05$) and plaque frequency (856/mm^2 *APOE3/3* versus 1113/mm^2 *APOE4/4*; $P < 0.05$) were significantly reduced in the hippocampi of the *APOE3/3* group compared to the *APOE4/4* group (Figure 7B). *APOE* genotype effects were less apparent in cerebral cortex, where plaque frequency (1822/mm^2 *APOE3/3* versus 2027/mm^2 *APOE4/4*; $P < 0.05$) was lower in *APOE3/3* recipients, but there was no significant effect of donor *APOE* genotype on total area occupied by plaques (Figure 7B). Average plaque size was not affected by donor genotype in either cortex or hippocampus (Supplemental Figure S2, A and B). When we examined adjacent sections with immunofluorescence, we found qualitatively more BM-derived cells in association with

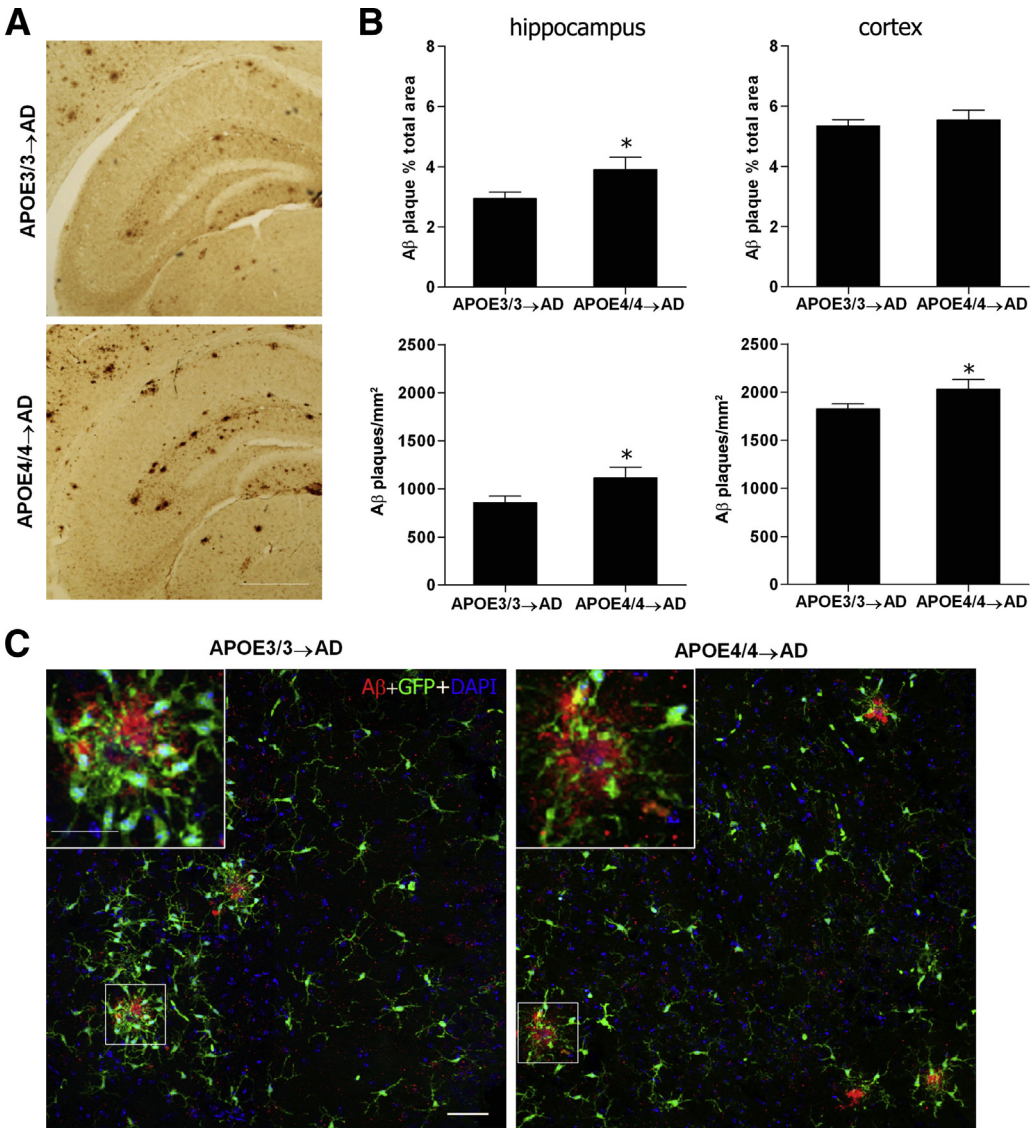

Figure 7 Quantification of Aβ plaque burden in *APOE3/3*;GFP versus *APOE4/4*;GFP-recipient *APPswe/PS1ΔE9* mice. **A**: Immunohistochemical stains for Aβ in hippocampus from 13-month-old chimeric mice 8 months post-transplantation reveal reduced plaque in *APOE3/3*;GFP-recipient mice compared with *APOE4/4*;GFP recipients. Scale bar = 500 μm. **B**: Quantitative analysis using standard thresholding techniques reveals significantly reduced area plaque density in cortex and in total area occupied by plaque as well as plaque density in hippocampus in *APOE3/3*;GFP-recipient mice compared with *APOE4/4*;GFP recipients. *$P < 0.05$, unpaired Student's *t*-test. Data are means ± SEM, $n = 8$ to 11. **C**: Confocal image analysis of representative brain sections stained for Aβ (red), GFP fluorescence (green), and DAPI (blue) reveal increased plaque-associated BMT-derived cells in *APPswe/PS1ΔE9* mice transplanted with *APOE3/3*;GFP (**inset**) versus *APOE4/4*;GFP BM (**inset**). Scale bars: 20 μm; 50 μm (**insets**).

Aβ plaques in the hippocampi of *APOE3/3* chimeras compared with *APOE4/4* (Figure 7C). In both groups, GFP^+ cells around plaques exhibited a less ramified morphology, with blunted processes extending around and into the immunopositive amyloid core (Figure 7C).

We further characterized Aβ burden in these mice using sequential extraction of Tris/HCl buffer− and guanidine-soluble Aβ. We found no significant differences in Tris/HCl buffer−soluble $Aβ_{40}$ or $Aβ_{42}$ between the two groups in cerebral cortex or hippocampus (Supplemental Figure S3, A and B). However, *APOE3/3* BMT recipients contained significantly less guanidine-soluble $Aβ_{40}$ in cerebral cortex and hippocampus compared with mice that received *APOE4/4* ($P < 0.05$) (Figure 8, A and B). There was no significant effect of donor *APOE* genotype on levels of guanidine-soluble $Aβ_{42}$ in cortex or hippocampus (Figure 8, A and B).

CNS Immune Modulation

TNF-α and MIF, cytokines that are elevated in patients with AD, and key activators of microglia-mediated neurotoxicity, were measured in cerebral cortex using real-time PCR. Both TNF-α and MIF concentrations were significantly elevated in *APOE4/4* compared to *APOE3/3* recipients (Figure 9A). By contrast, levels of IL-10, a cytokine that suppresses the actions of proinflammatory cytokine production and is associated

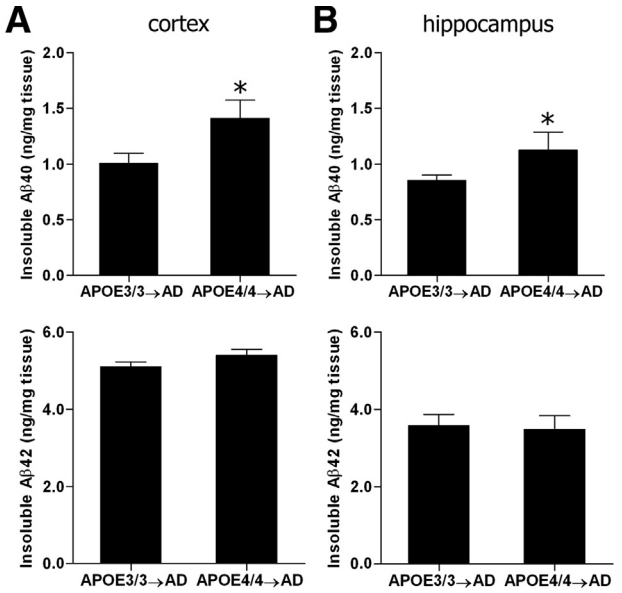

Figure 8 **A** and **B**: Quantification of Aβ species in BMT-recipient mice. A portion of cerebral cortex and whole hippocampus from 13-month-old BMT-recipient mice euthanized 8 months post-transplant and then perfused with ice-cold PBS were homogenized and sequentially dissolved in Tris-HCl buffer followed by 5 mol/L guanidine, and the lysates were then subjected to Luminex assay for Aβ species. Lysates in Tris-HCl buffer showed no donor *APOE* genotype—dependent differences in Aβ concentration (Supplemental Figure S3), but there was a significant reduction in cortical (**A**) and hippocampal (**B**) guanidine soluble (insoluble) $A\beta_{40}$ in *APOE3/3*;GFP BMT recipients compared with *APOE4/4*;GFP recipients. $^*P < 0.05$, unpaired Student's *t*-test. No significant differences were identified in $A\beta_{42}$ levels in cortex or hippocampus between different donor *APOE* genotypes. Data are means ± SEM, $n = 8$ to 11.

with a pro-phagocytic phenotype,[43,44] were lower in the *APOE4/4* group (Figure 9A). Donor *APOE* genotype did not promote differences in cerebral cortex expression of IL-6, IL-4, CCL2, CX3CL1, and CCL8 (Supplemental Figure S4). MHC class II has been shown to be increased in BMT-derived microglia, which we confirmed in both *APOE3/3*- and *APOE4/4*-derived microglia in this study in comparison with endogenous cells ($P < 0.01$ for *APOE3/3* microglia and $P < 0.05$ for *APOE4/4* microglia) (Figure 9B). However, there was no effect of donor *APOE* genotype on MHC class II expression. We found that chemokine receptor CCR2 was up-regulated in donor-derived microglia compared with endogenous microglia ($P < 0.05$) (Figure 9B), but again, we found no effect of *APOE*. Microglia origin (host versus donor) and genotype (*APOE3* versus *APOE4*) had no effect on expression of microglial complement receptor C5a or chemokine receptors CX3CR1 or CCR1 (Supplemental Figure S5). Overall, these results indicate that *APOE4/4* BMT resulted in a more proinflammatory state in cerebral cortex and hippocampus than did *APOE3/3*.

Discussion

Here, we tested the hypothesis that BMT with *APOE3*- or *APOE4*-expressing donor cells has both behavioral and neuropathological consequences in a mouse model of AD. Following previous work that optimized the age and duration of BMT,[24] we performed our experiments using *APOE3/3*;GFP or *APOE4/4*;GFP donor cells and 5-month-old *APPswe/PS1ΔE9* transgenic recipient mice 24 hours following myeloablative BMT with 10.5-Gy whole-body irradiation, and concluded our experiments at 8 months post-BMT (13 months of age). Using GFP allowed us to focus exclusively on apoE isoforms derived from BM donor cells because other cellular sources of mouse apoE remained intact in the recipient mice. We selected this approach, rather than using APOE-null mice, to better model the potential clinical situation if this approach were to prove to be successful in experimental models.

We demonstrated that hematological engraftment by *APOE3/3* or *APOE4/4* BM was nearly complete and that blood cell differentiation, including monocytes, was similar for these two groups except for proportionately greater numbers of CD11b monocyte/macrophage lineage cells in *APOE3/3* recipients. Perhaps related, the total number of microglia/monocytes in cerebral cortex and hippocampus were not significantly changed by BMT, but the replacement of resident cells was approximately half with *APOE3/3* BM compared to approximately one-third with *APOE4/4* BM. As with our previous experiments, we observed only BM-derived microglia/monocytes in brain parenchyma; no astrocytes or neurons were observed. Importantly, *APOE3/3* recipients also had improved habituation and spatial working memory compared to *APOE4/4* recipients. Finally we pursued several, potentially interrelated, mechanisms of action and showed that *APOE3/3* recipients had increased apoE tissue concentration, reduced burden of some forms of cerebral Aβ, and a relatively anti-inflammatory environment compared to *APOE4/4* recipients.

The BMT strategy used necessarily constrained our experimental design and thus final interpretation, rendering precise mechanistic interpretation difficult. Indeed, the *APOE3/3*-specific effects observed here could be mediated by differences in apoE concentration, intrinsic isoform-specific activities, relevant *APOE* genotype—dependent phenotypic differences in microglia, or some complex combination of these or other unsuspected interactions. Importantly, direct and indirect modulation of brain apoE has been shown to influence Aβ trafficking, cerebral Aβ concentration and plaque density, and local innate immune responses in a variety of mouse models.[4,5,8–10] Because reduction of Aβ plaque density and Aβ tissue concentration correlate with improved performance on behavioral tests in mice, one interpretation of our results is that BMT with *APOE3/3* led to increased cerebral apoE concentration, resulting in reduced Aβ accumulation and suppressed neuroinflammation that together improved behavioral test performance. How might BMT with *APOE3/3* have selectively increased cerebral cortical and hippocampal concentration of apoE? Because virtually all donor cells in cerebrum were microglia/monocytes, one possibility is that engrafted *APOE3/3* microglia secreted more apoE. Indeed,

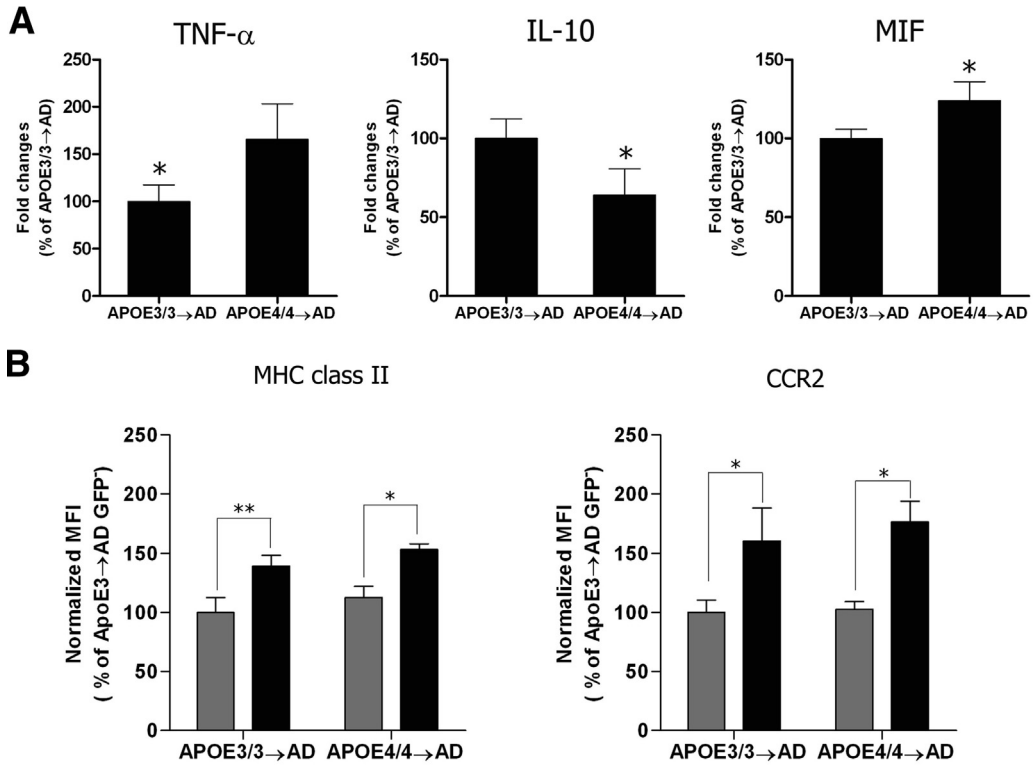

Figure 9 Alterations in innate immune molecular phenotype in BMT-recipient mice. **A:** Cortical tissue from 13-month-old mice that received BMT 8 months before sacrifice and were transcardially perfused with ice-cold PBS was flash frozen at the time of euthanasia, and RNA was isolated for qPCR analysis of inflammatory markers. Qualitative quantification was performed for each transcript. A decrease of mRNA levels in TNF-α and MIF and an increase in IL-10 mRNA levels was found in mice transplanted with *APOE3/3*;GFP BMCs compared with the chimeras that received *APOE4/4*;GFP BMCs. $*P < 0.05$, unpaired Student's *t*-test. All results are expressed as means ± SEM, $n = 7$ to 11. **B:** Mononuclear cells were isolated from cortex adjacent to that used for qPCR in the same mice. The cells (isolated with Percoll gradient) were resuspended and subjected to flow cytometric analysis for identification of donor ($GFP^+CD11b^+CD45^{low}$) and host ($GFP^-CD11b^+CD45^{low}$) microglial expression of innate immune effector molecules. Comparison of mean fluorescence intensity (MFI) in endogenous (GFP^-, grey bars) and donor (GFP^+, black bars) microglia for MHC class II and CCR2 revealed a significant reduction in both cell-surface proteins in endogenous versus donor cells, but no effect of donor *APOE* genotype. $**P < 0.01$, $*P < 0.05$, two-way analysis of variance analysis was performed using the Bonferroni *post hoc* test. MFIs were normalized to GFP^- microglia from *APOE3/3*;GFP→*APPswe/PS1ΔE9* chimeras for every phenotype. All results are expressed as means ± SEM, $n = 8$ to 11.

numerous studies have been performed to assess apoE protein levels in human serum,[45] cerebrospinal fluid,[46] and brain[47,48]; all have shown greater apoE concentration in the *APOE3* compared to the *APOE4* background. Although our results from primary astrocytes were consonant with these data, primary microglia showed the opposite relationship to *APOE* with greater secretion by *APOE4/4* than *APOE3/3* microglia, making this potential explanation for increased apoE in *APOE3/3* recipients unlikely. Further complicating such assessments is the potential for subtle interaction between donor-derived and resident host microglial populations resulting from incomplete central engraftment. In addition, whereas donor-derived microglia express human apoE isoforms, the AD host mice themselves express mouse apoE, creating a complex chimeric environment, the effects of which remain difficult to assess. Alternatively, the *APOE* genotype–dependent differential engraftment observed may have influenced Aβ deposition independent of brain apoE levels or in concert with the observed differences. Another potential explanation was that myeloablative BMT had permanently damaged the blood–brain barrier to permit abnormal transit of peripheral apoE into brain parenchyma. This also seems unlikely because previous studies have shown that the blood–brain barrier functions normally with respect to albumin and immunoglobulin after 10-Gy myeloablative BMT in C57BL/6 mice.[49] A potential explanation consistent with these and others' data are that increased cerebral apoE in *APOE3/3* recipients involves paracrine interactions between engrafted microglia/monocytes and resident cells, likely astrocytes, yielding increased tissue apoE concentration. Although the precise mechanism for the observed effects in transplanted mice remains unclear, it is important to note that AD animals received selective benefit from adoptive transfer of *APOE3/3* BM-derived cells, further supporting this novel therapeutic strategy.

In contrast to apoE and albumin, Aβ does cross the blood–brain barrier, and its degradation or transport by cells outside the CNS forms the basis of the sink hypothesis for Aβ clearance.[50] Because *APOE3/3* recipients had relatively increased differentiation to $CD11b^+$ peripheral monocytes/macrophages, a second possible explanation for our behavioral and neuropathological outcomes following BMT is enhanced peripheral clearance of Aβ by the larger pool of $CD11b^+$ monocytes/macrophages, with the increased,

remotely mediated clearance of Aβ responsible for reduced neuroinflammation and improved behavioral performance. To resolve the relative contribution of CNS versus peripheral BMT-derived cells on our behavioral and neuropathological endpoints, we are developing protocols for selective peripheral or central engraftment.

APOE is associated, not only with AD, but also with poorer clinical outcome in traumatic brain injury,[51] cognition in Parkinson disease,[52] multiple sclerosis,[53] and other neurological conditions, each of which has a significant inflammatory component. The data presented here suggest that BMT-derived central and/or peripheral cells that express *APOE3* modulate behavior and neuropathological changes in a mouse model of AD to a greater extent than those expressing *APOE4*. Although the toxicity of myeloablative BMT limits its clinical application primarily to malignancies, clinical trials for non-myeloablative BMT for noncancerous disease, such as multiple sclerosis and diabetes, are currently used in outpatient settings and offer hope that BMT might someday be adapted to be a potential therapeutic option for chronic neurological diseases.

Acknowledgments

We thank Samantha Rice, Meilany Wijaya, Dr. Carole Wilson, Dr. Elaine Raines, and Dr. Aru Arumuganathan (Benaroya Research Institute) for expert technical assistance and Aimee Schantz and Amy Look for administrative support.

Supplemental Data

Supplemental material for this article can be found at *http://dx.doi.org/10.1016/j.ajpath.2013.05.009*.

References

1. Naj AC, Jun G, Beecham GW, Wang LS, Vardarajan BN, Buros J, et al: Common variants at MS4A4/MS4A6E. CD2AP, CD33 and EPHA1 are associated with late-onset Alzheimer's disease. Nat Genet 2011, 43:436−441
2. Samuels SC, Silverman JM, Marin DB, Peskind ER, Younki SG, Greenberg DA, Schnur E, Santoro J, Davis KL: CSF beta-amyloid, cognition, and APOE genotype in Alzheimer's disease. Neurology 1999, 52:547−551
3. Schmechel DE, Saunders AM, Strittmatter WJ, Crain BJ, Hulette CM, Joo SH, Pericak-Vance MA, Goldgaber D, Roses AD: Increased amyloid beta-peptide deposition in cerebral cortex as a consequence of apolipoprotein E genotype in late-onset Alzheimer disease. Proc Natl Acad Sci U S A 1993, 90:9649−9653
4. Cramer PE, Cirrito JR, Wesson DW, Lee CY, Karlo JC, Zinn AE, Casali BT, Restivo JL, Goebel WD, James MJ, Brunden KR, Wilson DA, Landreth GE: ApoE-directed therapeutics rapidly clear beta-amyloid and reverse deficits in AD mouse models. Science 2012, 335:1503−1506
5. Kim J, Eltorai AE, Jiang H, Liao F, Verghese PB, Kim J, Stewart FR, Basak JM, Holtzman DM: Anti-apoE immunotherapy inhibits amyloid accumulation in a transgenic mouse model of Abeta amyloidosis. J Exp Med 2012, 209:2149−2156
6. Jiang Q, Lee CY, Mandrekar S, Wilkinson B, Cramer P, Zelcer N, Mann K, Lamb B, Willson TM, Collins JL, Richardson JC, Smith JD, Comery TA, Riddell D, Holtzman DM, Tontonoz P, Landreth GE: ApoE promotes the proteolytic degradation of Abeta. Neuron 2008, 58:681−693
7. Zhao L, Lin S, Bales KR, Gelfanova V, Koger D, Delong C, Hale J, Liu F, Hunter JM, Paul SM: Macrophage-mediated degradation of beta-amyloid via an apolipoprotein E isoform-dependent mechanism. J Neurosci 2009, 29:3603−3612
8. Deane R, Sagare A, Hamm K, Parisi M, Lane S, Finn MB, Holtzman DM, Zlokovic BV: apoE isoform-specific disruption of amyloid beta peptide clearance from mouse brain. J Clin Invest 2008, 118:4002−4013
9. Castellano JM, Kim J, Stewart FR, Jiang H, DeMattos RB, Patterson BW, Fagan AM, Morris JC, Mawuenyega KG, Cruchaga C, Goate AM, Bales KR, Paul SM, Bateman RJ, Holtzman DM: Human apoE isoforms differentially regulate brain amyloid-beta peptide clearance. Sci Transl Med 2011, 3:89ra57
10. Sharman MJ, Morici M, Hone E, Berger T, Taddei K, Martins IJ, Lim WL, Singh S, Wenk MR, Ghiso J, Buxbaum JD, Gandy S, Martins RN: APOE genotype results in differential effects on the peripheral clearance of amyloid-beta42 in APOE knock-in and knock-out mice. J Alzheimers Dis 2010, 21:403−409
11. Perlmutter LS, Scott SA, Barron E, Chui HC: MHC class II-positive microglia in human brain: association with Alzheimer lesions. J Neurosci Res 1992, 33:549−558
12. el Hachimi KH, Foncin JF: Do microglial cells phagocyte the beta/A4-amyloid senile plaque core of Alzheimer disease? C R Acad Sci III 1994, 317:445−451
13. DeWitt DA, Perry G, Cohen M, Doller C, Silver J: Astrocytes regulate microglial phagocytosis of senile plaque cores of Alzheimer's disease. Exp Neurol 1998, 149:329−340
14. Zhu Y, Nwabuisi-Heath E, Dumanis SB, Tai LM, Yu C, Rebeck GW, LaDu MJ: APOE genotype alters glial activation and loss of synaptic markers in mice. Glia 2012, 60:559−569
15. Maezawa I, Maeda N, Montine TJ, Montine KS: Apolipoprotein E-specific innate immune response in astrocytes from targeted replacement mice. J Neuroinflammation 2006, 3:10
16. Chen S, Averett NT, Manelli A, Ladu MJ, May W, Ard MD: Isoform-specific effects of apolipoprotein E on secretion of inflammatory mediators in adult rat microglia. J Alzheimers Dis 2005, 7: 25−35
17. Vitek MP, Brown CM, Colton CA: APOE genotype-specific differences in the innate immune response. Neurobiol Aging 2009, 30: 1350−1360
18. Maezawa I, Nivison M, Montine KS, Maeda N, Montine TJ: Neurotoxicity from innate immune response is greatest with targeted replacement of E4 allele of apolipoprotein E gene and is mediated by microglial p38MAPK. FASEB J 2006, 20:797−799
19. Cudaback E, Li X, Montine KS, Montine TJ, Keene CD: Apolipoprotein E isoform-dependent microglia migration. FASEB J 2011, 25: 2082−2091
20. Brown CM, Choi E, Xu Q, Vitek MP, Colton CA: The APOE4 genotype alters the response of microglia and macrophages to 17beta-estradiol. Neurobiol Aging 2008, 29:1783−1794
21. Priller J, Flugel A, Wehner T, Boentert M, Haas CA, Prinz M, Fernandez-Klett F, Prass K, Bechmann I, de Boer BA, Frotscher M, Kreutzberg GW, Persons DA, Dirnagl U: Targeting gene-modified hematopoietic cells to the central nervous system: use of green fluorescent protein uncovers microglial engraftment. Nat Med 2001, 7:1356−1361
22. Simard AR, Rivest S: Bone marrow stem cells have the ability to populate the entire central nervous system into fully differentiated parenchymal microglia. FASEB J 2004, 18:998−1000
23. Simard AR, Soulet D, Gowing G, Julien JP, Rivest S: Bone marrow-derived microglia play a critical role in restricting senile plaque formation in Alzheimer's disease. Neuron 2006, 49:489−502

24. Keene CD, Chang RC, Lopez-Yglesias AH, Shalloway BR, Sokal I, Li X, Reed PJ, Keene LM, Montine KS, Breyer RM, Rockhill JK, Montine TJ: Suppressed accumulation of cerebral amyloid {beta} peptides in aged transgenic Alzheimer's disease mice by transplantation with wild-type or prostaglandin E2 receptor subtype 2-null bone marrow. Am J Pathol 2010, 177:346−354
25. Xu PT, Schmechel D, Rothrock-Christian T, Burkhart DS, Qiu HL, Popko B, Sullivan P, Maeda N, Saunders AM, Roses AD, Gilbert JR: Human apolipoprotein E2. E3, and E4 isoform-specific transgenic mice: human-like pattern of glial and neuronal immunoreactivity in central nervous system not observed in wild-type mice. Neurobiol Dis 1996, 3:229−245
26. Sullivan PM, Mezdour H, Aratani Y, Knouff C, Najib J, Reddick RL, Quarfordt SH, Maeda N: Targeted replacement of the mouse apolipoprotein E gene with the common human APOE3 allele enhances diet-induced hypercholesterolemia and atherosclerosis. J Biol Chem 1997, 272:17972−17980
27. Borchelt DR, Ratovitski T, van Lare J, Lee MK, Gonzales V, Jenkins NA, Copeland NG, Price DL, Sisodia SS: Accelerated amyloid deposition in the brains of transgenic mice coexpressing mutant presenilin 1 and amyloid precursor proteins. Neuron 1997, 19: 939−945
28. Vehmas AK, Borchelt DR, Price DL, McCarthy D, Wills-Karp M, Peper MJ, Rudow G, Luyinbazi J, Siew LT, Troncoso JC: beta-Amyloid peptide vaccination results in marked changes in serum and brain Abeta levels in APPswe/PS1DeltaE9 mice, as detected by SELDI-TOF-based ProteinChip technology. DNA Cell Biol 2001, 20:713−721
29. Li X, Cudaback E, Keene CD, Breyer RM, Montine TJ: Suppressed microglial E prostanoid receptor 1 signaling selectively reduces tumor necrosis factor alpha and interleukin 6 secretion from toll-like receptor 3 activation. Glia 2011, 59:569−576
30. Li X, Cudaback E, Breyer RM, Montine KS, Keene CD, Montine TJ: Eicosanoid receptor subtype-mediated opposing regulation of TLR-stimulated expression of astrocyte glial-derived neurotrophic factor. FASEB J 2012, 26:3075−3083
31. Amador-Arjona A, Elliott J, Miller A, Ginbey A, Pazour GJ, Enikolopov G, Roberts AJ, Terskikh AV: Primary cilia regulate proliferation of amplifying progenitors in adult hippocampus: implications for learning and memory. J Neurosci 2011, 31:9933−9944
32. Cardona AE, Huang D, Sasse ME, Ransohoff RM: Isolation of murine microglial cells for RNA analysis or flow cytometry. Nat Protoc 2006, 1:1947−1951
33. Anglen CS, Truckenmiller ME, Schell TD, Bonneau RH: The dual role of CD8+ T lymphocytes in the development of stress-induced herpes simplex encephalitis. J Neuroimmunol 2003, 140:13−27
34. Campanella M, Sciorati C, Tarozzo G, Beltramo M: Flow cytometric analysis of inflammatory cells in ischemic rat brain. Stroke 2002, 33: 586−592
35. Ford AL, Goodsall AL, Hickey WF, Sedgwick JD: Normal adult ramified microglia separated from other central nervous system macrophages by flow cytometric sorting. Phenotypic differences defined and direct ex vivo antigen presentation to myelin basic protein-reactive CD4+ T cells compared. J Immunol 1995, 154: 4309−4321
36. Havenith CE, Askew D, Walker WS: Mouse resident microglia: isolation and characterization of immunoregulatory properties with naive CD4+ and CD8+ T-cells. Glia 1998, 22:348−359
37. Keene CD, Chang R, Stephen C, Nivison M, Nutt SE, Look A, Breyer RM, Horner PJ, Hevner R, Montine TJ: Protection of hippocampal neurogenesis from toll-like receptor 4-dependent innate immune activation by ablation of prostaglandin E2 receptor subtype EP1 or EP2. Am J Pathol 2009, 174:2300−2309
38. Quinn JF, Bussiere JR, Hammond RS, Montine TJ, Henson E, Jones RE, Stackman RW Jr: Chronic dietary alpha-lipoic acid reduces deficits in hippocampal memory of aged Tg2576 mice. Neurobiol Aging 2007, 28:213−225
39. Mildner A, Schmidt H, Nitsche M, Merkler D, Hanisch UK, Mack M, Heikenwalder M, Bruck W, Priller J, Prinz M: Microglia in the adult brain arise from Ly-6ChiCCR2+ monocytes only under defined host conditions. Nat Neurosci 2007, 10:1544−1553
40. Saura J, Petegnief V, Wu X, Liang Y, Paul SM: Microglial apolipoprotein E and astroglial apolipoprotein J expression in vitro: opposite effects of lipopolysaccharide. J Neurochem 2003, 85: 1455−1467
41. O'Leary TP, Brown RE: Visuo-spatial learning and memory deficits on the Barnes maze in the 16-month-old APPswe/PS1dE9 mouse model of Alzheimer's disease. Behav Brain Res 2009, 201:120−127
42. Lalonde R, Kim HD, Fukuchi K: Exploratory activity, anxiety, and motor coordination in bigenic APPswe + PS1/DeltaE9 mice. Neurosci Lett 2004, 369:156−161
43. Smith ME, van der Maesen K, Somera FP: Macrophage and microglial responses to cytokines in vitro: phagocytic activity, proteolytic enzyme release, and free radical production. J Neurosci Res 1998, 54: 68−78
44. Szczepanik AM, Funes S, Petko W, Ringheim GE: IL-4. IL-10 and IL-13 modulate A beta(1−42)-induced cytokine and chemokine production in primary murine microglia and a human monocyte cell line. J Neuroimmunol 2001, 113:49−62
45. Panza F, Solfrizzi V, Colacicco AM, Basile AM, D'Introno A, Capurso C, Sabba M, Capurso S, Capurso A: Apolipoprotein E (APOE) polymorphism influences serum APOE levels in Alzheimer's disease patients and centenarians. Neuroreport 2003, 14:605−608
46. Pirttila T, Koivisto K, Mehta PD, Reinikainen K, Kim KS, Kilkku O, Heinonen E, Soininen H, Riekkinen P Sr, Wisniewski HM: Longitudinal study of cerebrospinal fluid amyloid proteins and apolipoprotein E in patients with probable Alzheimer's disease. Neurosci Lett 1998, 249:21−24
47. Bertrand P, Poirier J, Oda T, Finch CE, Pasinetti GM: Association of apolipoprotein E genotype with brain levels of apolipoprotein E and apolipoprotein J (clusterin) in Alzheimer disease. Brain Res Mol Brain Res 1995, 33:174−178
48. Riddell DR, Zhou H, Atchison K, Warwick HK, Atkinson PJ, Jefferson J, Xu L, Aschmies S, Kirksey Y, Hu Y, Wagner E, Parratt A, Xu J, Li Z, Zaleska MM, Jacobsen JS, Pangalos MN, Reinhart PH: Impact of apolipoprotein E (ApoE) polymorphism on brain ApoE levels. J Neurosci 2008, 28:11445−11453
49. Lampron A, Lessard M, Rivest S: Effects of myeloablation, peripheral chimerism, and whole-body irradiation on the entry of bone marrow-derived cells into the brain. Cell Transplant 2012, 21: 1149−1159
50. Zhang Y, Lee DH: Sink hypothesis and therapeutic strategies for attenuating Abeta levels. Neuroscientist 2011, 17:163−173
51. Friedman G, Froom P, Sazbon L, Grinblatt I, Shochina M, Tsenter J, Babaey S, Yehuda B, Groswasser Z: Apolipoprotein E-epsilon4 genotype predicts a poor outcome in survivors of traumatic brain injury. Neurology 1999, 52:244−248
52. Tsuang D, Leverenz JB, Lopez OL, Hamilton RL, Bennett DA, Schneider JA, Buchman AS, Larson EB, Crane PK, Kaye JA, Kramer P, Woltjer R, Trojanowski JQ, Weintraub D, Chen-Plotkin AS, Irwin DJ, Rick J, Schellenberg GD, Watson GS, Kukull W, Nelson PT, Jicha GA, Neltner JH, Galasko D, Masliah E, Quinn JF, Chung KA, Yearout D, Mata IF, Wan JY, Edwards KL, Montine TJ, Zabetian CP: APOE ε4 increases risk for dementia in pure synucleinopathies. JAMA Neurol 2013, 70:223−228
53. Chapman J, Vinokurov S, Achiron A, Karussis DM, Mitosek-Szewczyk K, Birnbaum M, Michaelson DM, Korczyn AD: APOE genotype is a major predictor of long-term progression of disability in MS. Neurology 2001, 56:312−316